Geosynthetics - 7th ICG - Delmas, Gourc & Girard (eds) © 2002 Swets & Zeitlinger, Lisse ISBN 90 5809 523 1

Creep behavior of embedded HDPE geomembrane liner in waste landfill

T. NISHIGATA, KansaiUniversity, Japan
K. NISHIDA, Kansai University, Japan

ABSTRACT: In this study, the creep characteristics of high-density polyethylene (HDPE) geomembrane sheets subjected to differential settlement of foundations in waste land fill were investigated. The creep characteristics of each geomembrane specimen were assessed under multi-axial tensile stress. The reduction factor of tensile strength reflecting the influence of creep deformation of geomembrane is proposed for application to the actual design process.

1 INTRODUCTION

According to a recent report, local settlement of foundations at the beneath a geomembrane liner may result in the destruction of the geomembrane. Therefore, it is essential to study the long-term strength and deformation characteristics of geomembranes in foundations after the completion of construction. Nomoto et al. (2000) studied the deformation behavior of geomembranes using a two-dimensional model with the trap door test apparatus. Levacher et. Al (1994), Soong et al.(1994), and Farrag et al. (1997) also studied the creep characteristics of geomembranes using the uniaxial tensile test. However, multi-axial tensile stress may act on the geomembrane near the location of the local deformation. Natsuka (1999) pointed out that the load condition greatly affects the tensile strength characteristics of the geomembrane.

We studied the creep deformation characteristics of high-density polyethylene (HDPE) geomembrane under a condition of multi-axial tensile stress and discuss a method for applying knowledge of the creep deformation to the actual design by introducing the reduction factor of the tensile strength of the geomembrane.

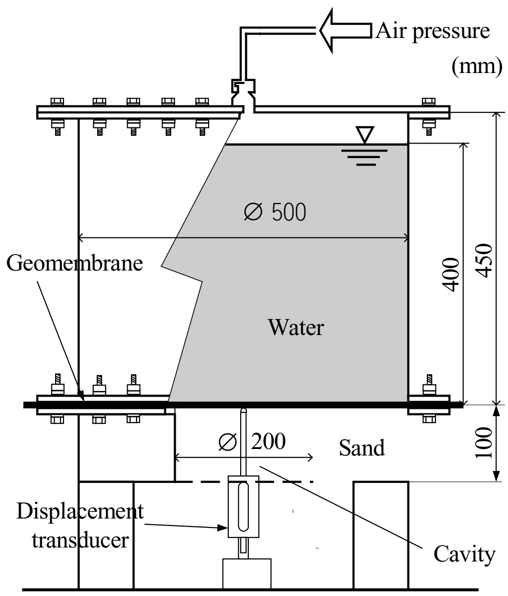

Figure 1. Test apparatus.

2 EXPERIMENTAL EQUIPMENT AND TEST METHOD

Figure 1 shows the experimental equipment used for the creep test. This equipment is a circular soil tank with a diameter of 50 cm, a height of 45 cm and a 20 cm diameter cavity at the base to simulate local settlement. Geomembrane specimens were placed over the cavity and load was applied by air pressure from upper side. This test condition produced a multi-axial tensile load on the geomembrane specimen. A displacement transducer was installed in the lower part of the cavity to measure the expanded deformation of the geomembrane. As shown in Fig.2, strain gages were attached to the points of 0, 2, 4, 6, 8, 12, 16, and 24 cm from the center of geomembrane sample to measure the tensile strain at each point. The temperature was maintained at 22ºC during the creep test.

Three HDPE geomembrane samples with different thicknesses were used for the creep tests, as shown in Table 1. The table also shows the mechanical properties of the samples as measured using a uniaxial tensile test.

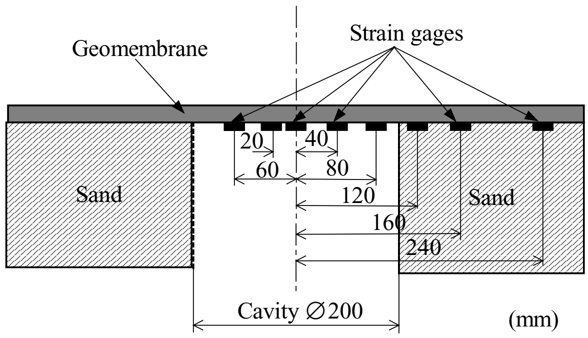

Figure 2. Locations of strain gages attached on geomembrane sample.

Table 1. Tensile properties of HDPE geomembrane samples.

Sample No.	1	2	3
Thickness (mm)	1.0	1.5	2.0
Tensile strength (MPa)	20.1	23.0	27.0
Ultimate strain (%)	780	860	940
Secant modulus at 10% strain (MPa)	160	140	120

Figures 3 to 5 show the test results on the three geomembrane specimens under the constant creep load. The legends in the figure indicate the positions of strain gage attachment (distances from the center). In any case, the tensile strain at the center is the greatest and decreases towards the edge. The tensile strain close

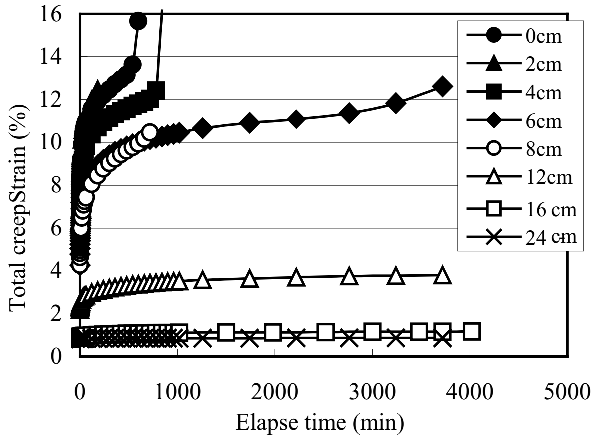

Figure 3. Creep test results of HDPE sample of 1.0mm thickness under σ_c=196kPa.

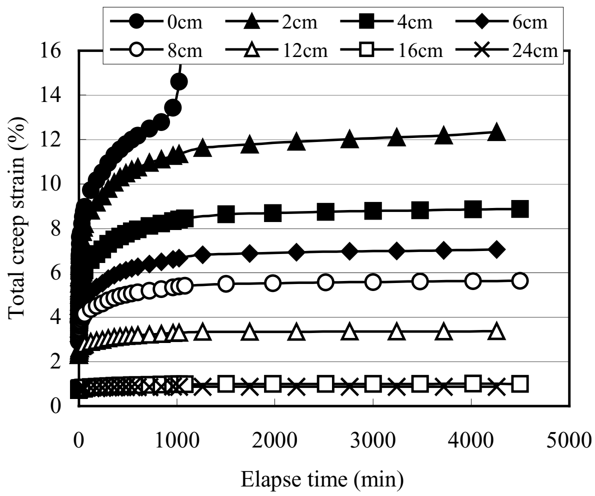

Figure 4. Creep test results of HDPE sample of 1.5mm thickness under σ_c=245kPa.

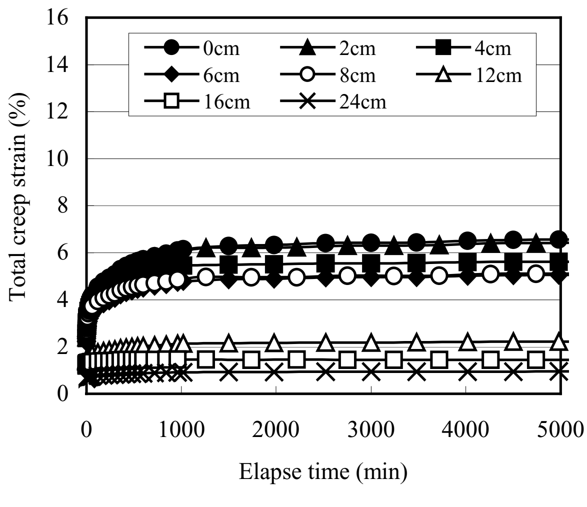

Figure 5. Creep test results of HDPE sample of 2.0mm thickness under σ_c=245kPa.

to the center of a thin geomembrane specimen showed rapid growth after the start of the test and reached the tertiary creep stage. The critical tensile strain upon reaching the tertiary stage is approximately 12% and almost equal at all points on the geomembrane specimen.

The result on the 1.5 mm thick geomembrane specimen shown in Fig.4, the creep deformation around the center reaches the tertiary stage and the critical tensile strain is also 12%. Each HDPE geomembrane specimen reaches the tertiary creep stage and causes rupture at the same critical creep strain, although the thickness differs. Regarding the 2.0 mm thick membrane specimen shown in Fig.5, the elongation strain seems to remain at about 6% in the secondary creep stage in the load range used in this experiment.

In a usual uniaxial tensile test of HDPE sheet, the strain needed to break down can be as large as several hundred percent, as shown in Table 1. Note that the critical deformation for reaching the tertiary creep stage is unexpectedly small under the condition of multi-axial tensile stress.

3 DEFORMATION CHARACTERISTICS OF GEOMEMBRANE IN A MULTI-TENSILE CONDITION

Under the experimental conditions used in this study, geomembrane specimen on the circular cavity shows spherical expansion deformations. This makes it necessary to clarify the relationship between the geomembrane tensile stress and strain under the multi-axial tensile stress. As shown in Fig.6, the geomembrane specimens on the circular cavity are assumed to be deformed into spherical crowns under an applied load. The average elongation strain and tensile stress generated on the geomembrane specimens deformed as illustrated in Fig.6 can be calculated by following equations (Natsuka (1999)).

$$\varepsilon = \frac{2\pi R\delta}{\pi (L/2)^2} - 1 = \frac{8R\delta}{L^2} - 1 \tag{1}$$

$$\sigma = \frac{(L^2 + 4\delta^2)}{4Ld\sin(\theta/2)} p \tag{2}$$

whereas, L: Cavity width, R : Radius of spherical crown, δ : Vertical settlement of the center, p : Applied load, and d : Thickness of the geomembrane specimen.

To validate the above formulas, the relationship between the vertical settlement at a center point of geomembrane specimen and the tensile strain at each point was checked using the equipment of Fig.1 under rapid loading (loading speed = 1 kPa/sec) by which the influence of creep deformation can be ignored.

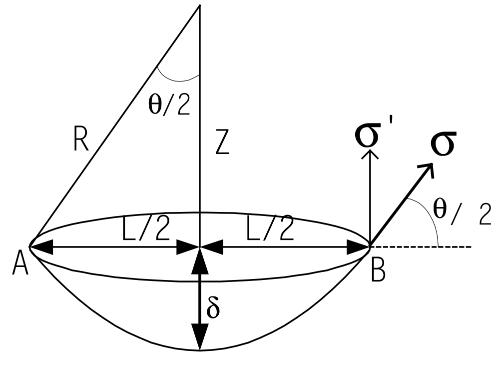

Figure 6. Schematic deformation of geomembrane located on cavity.

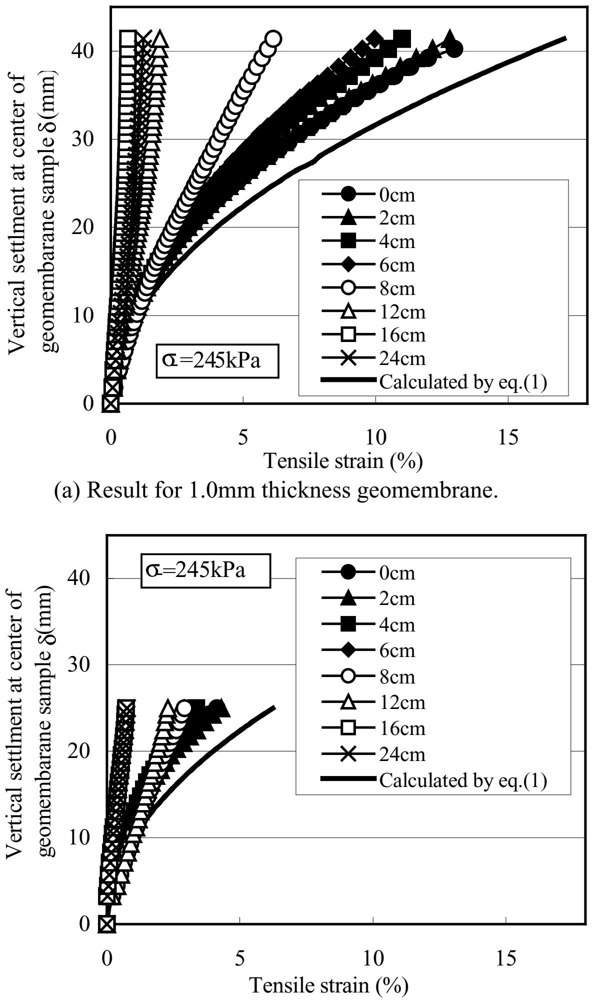

(a) Result for 1.0mm thickness geomembrane.

(b) Result for 1.5mm thickness geomembrane.

Figure 7. Relationship between the in-plane tensile strains and the vertical settlement at center point of geomembrane sample.

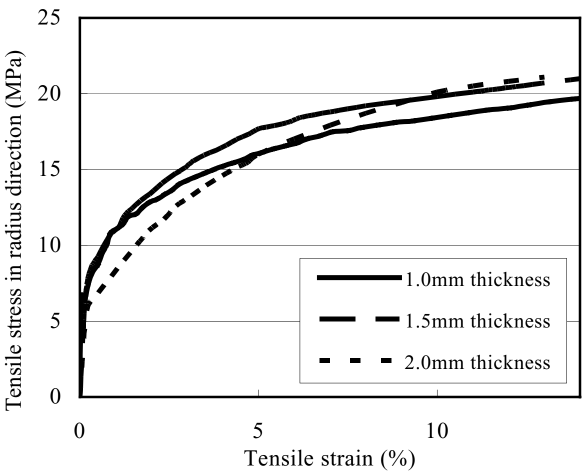

Figure 8. Stress-strain curves for HDPE geomembranes under multiple tensile condition.

Figure 7 shows the results of the experimental and calculated-strain of the geomembrane specimen obtained from the vertical settlement at the center. The calculated value of the strain is slightly greater than the measured ones. If this calculated value is regarded as a safety side, equation (1) is considered to be applicable to the prediction of the deformation of a geomembrane lining over a circular cavity.

Figure 8 shows the relationships between tensile stress and strain calculated from the vertical deformation at the center and the applied load *p* by using equations (1) and (2). Irrespective of the specimen thickness, similar stress strain curves were obtained. If these relationships are considered as the stress strain curve of the geomembrane under a multi-axial tensile stress, it can be determined that the secant tensile modulus at a strain of 10% is almost E_{10}=200 MPa and the initial tensile rigidity is E_0=3700 MPa. Comparing the values with the secant tensile modulus in the uniaxial tensile test in Table 1 indicates the value from the multi-axial tensile test is greater than that of uniaxial tensile.

4 REDUCTION FACTOR OF TENSILE STRENGTH DUE TO CREEP DEFORMATION

Once the creep characteristics of a material are clarified, it becomes important to understand how the characteristics should be introduced to the actual design. Since the basic strength of a geomembrane material is characterized by its tensile strength, it is effective to define a reduction factor of tensile strength for the application of the understanding of the creep characteristics of the geomembrane to the design procedure.

Therefore, we discuss the reduction factor due to creep by using the stress-strain curves under multi-axial tensile stress conditions (Fig.8) and the results obtained in the previous sections in which the critical creep strain to reach the tertiary creep stage was approximately 12%.

Figure 9 shows the method for the determination of the reduction factor. The tensile strain and the stress at each elapse time were obtained by using Eqs.(1) and (2) and the settlement ( ) at each elapse time (60, 600, and 6000 min) during the creep test. The three straight lines in the figure were drawn by connecting the points correspond to calculated stress and strain with the origin. These straight lines can be considered as representing the apparent tensile rigidity of the geomembrane specimen at the each elapsed time, and we can see that the tensile rigidity decreases with time. The figure shows that the tensile stresses

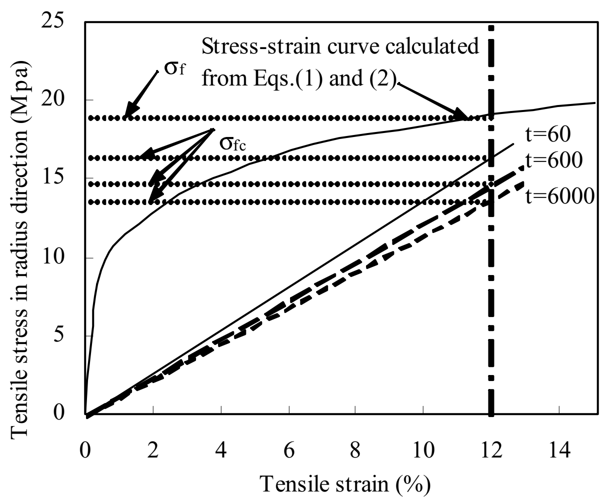

Figure 9. Definition of tensile strength reflecting the influence of the creep characteristics.

when the straight lines reach the critical strain (12%) were the apparent tensile strength (σ_{fc}) of the HDPE geomembrane reflecting the creep characteristics.

Figure 9 also shows the stress-strain curve for the 1 mm thick HDPE geomembrane specimen shown in Fig.8. Likewise, the tensile stress corresponding to the 12% strain on this curve is defined as the tensile strength (σ_f) under a condition of multi-axial stress. The ratio of the tensile strength (σ_{fc}/σ_f) is defined as the reduction factor of the tensile strength of a HDPE geomembrane reflecting the creep characteristics. Figure 10 shows the changes of the reduction factor with elapse time. The reduction factor seems to converge at about 0.6, irrespective of the thickness of the geomembrane. If only the material is the same, there seems no significant difference in the reduction factor of tensile strength. Therefore, multiplication the reduction factor (0.6) to geomembrane tensile strength for rapid loading will provide the long-term tensile strength reflecting the influence of the creep characteristics under multi-axial stress conditions and enable to apply to design as the long-term strength.

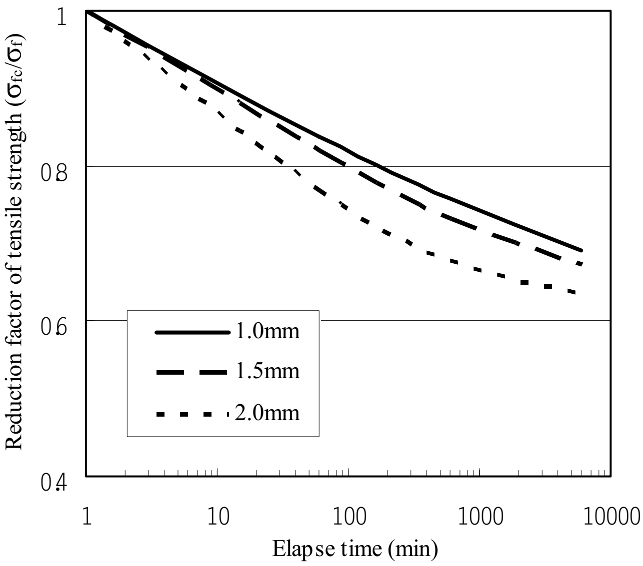

Figure 10. Change of Reduction factor with time.

5 CONCLUSION

(1) If the creep strain exceeds approximately 12%, the strain in the HDPE membrane increases rapidly irrespective of membrane thickness. Then, the creep deformation approaches the tertiary stage and causes rupture.

(2) The tensile strength characteristic of HDPE geomembrane under a multi-axial stress is different from that under a uniaxial stress. In particular, the tensile rigidity under a multi-axial stress may be slightly greater and indicate brittle fracture behavior.

(3) The reduction factor of tensile strength reflecting the creep characteristics was almost 0.6, and the value of the factor is irrespective of the thickness of the HDPE geomembrane. Therefore, the long-term strength of the HDPE geomembrane considering creep characteristic is approximately 60% of it's tensile strength.

PREFERENCES

Nomoto, T., Imaizumi, S., Abe, S., Tsuboi, M. and Futami, T. 2000. Modeled test for estimating the tensile behavior of embedded HDPE geomembrane subjected to differential settlement of base ground, *Jour. Of Geotechnical Eng., JSCE*, No.652, 35-45.

Natsuka, I. 1999. Reasonable application methods of geomembranes to the surface lining system of reservoir, *Geosynthetics Engineering Jour., Japan Chapter of IGS*, 370-379.

Levacher, D. & Blivet, J.C. 1994. Tensile and creep behavior of geotextiles, *Proc. of Fifth International Conference on Geotextiles, Geomembranes and Related Products,* 1131-1134.

Soong, T.Y. 1994. Effects of four experimental variables on the stress relaxation behavior of HDPE geomembranes, *Proc. of Fifth International Conference on Geotextiles, Geomembranes and Related Products*, 1139-1147.

Farrag, K. 1997. Prediction of long term strain of geosynthetics from accelerated creep tests, *Proc. of Geosynthetics'97 Conference,* 267-269.

Natsuka,O. 1999. Studies on design of surface lining system of dam and reservoirs, *National Research Institute of Agricultural Engineering*, No.38, 59-65.